

Computing Surface Acoustic Wave Dispersion and Band Gaps

Ryan S. Westafer*, Saeed Mohammadi, Ali Adibi, and William D. Hunt

School of Electrical and Computer Engineering, Georgia Institute of Technology

*Corresponding author: ryan.westafer@gatech.edu; 791 Atlantic Drive NW, Atlanta, GA 30332, USA

Abstract: The dispersion of surface acoustic waves (SAWs) has long been studied for diverse applications ranging from seismic waves to microelectronic filters. In this work, we apply COMSOL Multiphysics software for the finite element investigation of SAW dispersion in two inhomogeneous materials: (a) layered structures, and (b) periodically patterned layered structures known as surface phononic crystals (PnCs). Using the COMSOL Script interface and eigenfrequency analysis, we parametrically solve for surface wave modes versus the wave number, $k(\lambda)$. In validation against experimental data, we have devised a post-processing method to rank the many computed modes according to likelihood of experimental detection.

Keywords: SAW, FEM, dispersion, phononic crystal

1. Introduction

Surface acoustic waves (SAWs) were mathematically described by Lord Rayleigh in 1885. These waves are ideally constrained to the mechanically free interface of a solid and feature $r^{-1/2}$ propagation loss from a point source.

In the many years since, similar acoustic modes have been observed and modeled to propagate at the interfaces of arbitrary solid structures. The study of these waves is useful in seismology and other areas, but there is much recent interest in finite element simulation of high frequency electrical filters [1], and micro- or nano-fabrication-enabled sensors [2,3]. In some of the latest studies, techniques specially adapted from photonics have been applied to simulate and experimentally confirm acoustic bandgap devices [4, 5].

In this work, we demonstrate the utility of COMSOL Multiphysics and its MATLAB scripting interface to produce dispersion plots for some interesting problems featuring layered structures on silicon substrates. In practice, such layers are useful as transducing materials (silicon is not piezoelectric), high velocity acoustic waveguides, or sensing films. The structures are

inhomogeneous in one or more spatial dimensions.

2. Dispersion in Structures

We examine both layered structures with and without photolithographic patterning. While one case is nonuniform with depth, the other is nonuniform in both depth and width. Both of these inhomogeneous structures exhibit surface wave dispersion.

The different lossless materials used in these structures have different acoustic velocities, and as the wavelength changes, the distribution of energy among the materials changes. Energy is then transferred among modes according to wavelength, and a nonlinear *dispersive* relationship then exists between f , λ , and v . The resonant frequency and energy distribution depend upon wavelength. Loss *with respect to a certain mode* may be apparent though the materials are lossless.

In layered structures, the so-called “leaky” waves (LSAWs) couple to bulk modes, resulting in energy loss from the surface. In patterned layered structures, waves may encounter stop bands or pass bands (e.g. Bragg scattering), and it is even possible for mode coupling to occur such that a layered structure does not radiate bulk waves.

3. Mathematical Model

In this work, we use the finite element method (FEM), which typically adopts a relatively simple mathematical formulation of the problem such that intricacies are left to the computational domain: structure, material parameters, and boundaries.

3.1 Governing Equation

The problems we solve in this work follow closely from first-principles physics, namely Newton’s Second Law of motion. Equation (1) shows the structural mechanics formulation,

where \mathbf{u} is the solution vector containing displacements u_x and u_y . For our analysis, the equation is homogeneous, i.e. there is no independent forcing term, \mathbf{F} .

$$\rho \frac{\partial^2 \mathbf{u}}{\partial t^2} - \nabla \cdot \mathbf{c} \nabla \mathbf{u} = \mathbf{F} = 0 \quad (1)$$

3.2 Eigenvalue Problem

Assuming a time-harmonic (resonant, steady-state) solution is one way of finding persistent solutions having measurable lifetimes.

Equation (1) is Fourier transformed and the resulting harmonic time dependence, $\exp(i\omega t)$, is factored out, leaving $-\omega^2$ to replace the time derivative. This factor represents the eigenvalues we seek: the mode frequencies.

What remains is similar to equation (2) and may be solved as a linear algebra eigenvalue problem where the canonical matrix, \mathbf{A} , and solution, \mathbf{u} , vary over the subdomain(s) and boundaries.

$$\mathbf{A}\mathbf{u} = \phi\mathbf{u}; \mathbf{A} = \frac{\nabla \cdot \mathbf{c} \nabla}{\rho}; \phi = \omega^2 \quad (2)$$

The eigenvalues, ϕ , yield the mode frequencies. In our study, we use COMSOL Script to iteratively vary the structure and/or boundary conditions. In an effort to see the important modes, we collect many mode frequencies, typically 30 per wavelength. We then sort the results in a post-processing step.

3.3 Boundary Conditions

COMSOL Multiphysics will produce many solutions given the very general formulation of the problem. For instance, compare Lamb waves and Rayleigh waves in Figure 1. Whereas the Lamb waves are plate modes and have free upper and lower boundaries, the Rayleigh modes are single-surface modes which have a displacement profile decaying with depth into the substrate.

We seek Rayleigh-type solutions, so we enforce a typical rule of thumb for the penetration depth: two wavelengths [6]. Therefore, in every SAW simulation, we resize the structure to be 1.8 wavelengths tall and fix the bottom boundary to zero displacement: $u = 0$.

This is, of course, only an approximation to the ideal semi-infinite case.

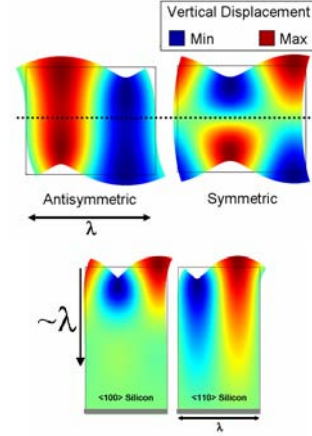


Figure 1. Lamb wave (plate mode, top), Rayleigh wave (surface mode, bottom). The structure scale corresponds to the acoustic wavelength, λ , but the deformations are not to scale.

Along the x -axis, we apply periodic boundary conditions. This is because we desire surface waves propagating parallel to the top surface, implying periodicity leftward and rightward. Thus the leftmost and rightmost boundaries and vertices share the state variables u (displacement), v (velocity), and also V (electrical potential) when appropriate. The assignment is shown in equation 3.

$$\begin{aligned} u_{x=0} &= u_{x=\lambda} \\ v_{x=0} &= v_{x=\lambda} \end{aligned} \quad (3)$$

In the case of a domain uniform in the x direction, this is sufficient; the structure period equals the solution period. For the periodically patterned structures, where in general the structure period does not equal the solution period, we will show an adjustment to the equation.

4. Use of COMSOL Multiphysics

Throughout this work, we apply the MEMS Module operating under the 2-D ‘‘Piezo Plane Strain (smppn)’’ Application Mode. The two-

dimensional mode is suitable because we assume infinite extent of the structure in the unused z direction. This has the added advantage of reducing the spatial domain to two dimensions. Figure 2 shows a patterned layer structure (one-dimensional surface PnC) and the 2-D computational domain in x and y directions only.

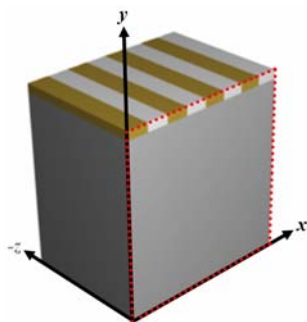


Figure 2. Example cross-sectional view of a patterned thin film on a substrate. The computational domain slice is enclosed with red dots.

We used unaltered material constants and tensors from the MEMS Module material library. The anisotropic or piezoelectric option was chosen where appropriate, e.g. single crystal silicon substrate or zinc oxide film, respectively.

The number of degrees of freedom (DOF) allowed in the models was at least 500 and at most 4,000 (piezoelectric film on silicon). The number of degrees of freedom was allowed to change in each iteration as the structure was scaled to accommodate nearly $2*\lambda$ penetration depth.

The simulation was run on several desktop personal computers running COMSOL 3.5a on Microsoft Windows XP Professional with 1+ GHz 32-bit processor and 1+ GB RAM. Each iteration required about one second, completing a typical dispersion plot or band diagram in thirty seconds to one minute, depending on the number of wave numbers (iterations).

4.1 Solver Parameters

The following are the settings used consistently through this work:

Solver Mode: Eigenfrequency Analysis
 Matrix Symmetry: Hermitian
 Eigenvalues: 30

We require the Hermitian condition because we later introduce complex-valued boundary conditions in the case of the periodically patterned layered structure. This structure requires additional modulation of the periodic boundary to enforce the solution period distinct from the structure period.

We allow a large number of modes, e.g. 30, over a wide frequency range because we are able to sort them and cull those irrelevant to experimental observation.

4.2 Meshing

This work was accomplished exclusively with default mesh settings. The adjoining rectangular subdomains used the “Triangular (Advancing Front)” mesh with Schlag quadratic elements. The number and size were determined automatically by COMSOL Multiphysics for re-meshing in each iteration.

4.3 COMSOL Script

It can be difficult to completely define a model geometry and mesh, configure the solver, and post-process solutions using COMSOL Script. The authors recommend the creation and solution of a model in COMSOL before saving as a MATLAB-compatible ‘.m’ file. The file can then be edited to include an iteration loop, plotting commands, etc. We found it helpful to recreate a model and solve it with the minimum number of steps and no mistakes, because COMSOL records a complete history of commands in the ‘.m’ file, regardless whether they are used.

Given the eigenproblem in section 3.2, we obtain the eigenvalue for the j th iteration using the following equation:

$$f = \frac{|\Im(fem.sol.lambda(j))|}{2\pi}. \quad (4)$$

As an iterative procedure, the script program accepts an array of wave vectors and other parameters specifying layer thickness and/or

phononic crystal parameters. The general script flow diagram is provided in Figure 3.

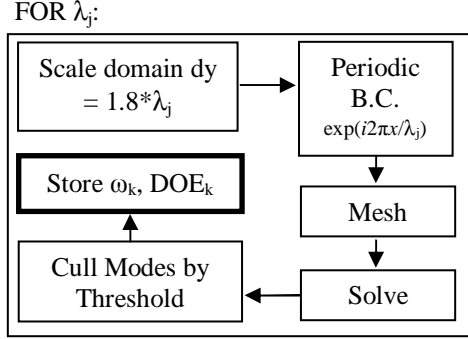


Figure 3. Script procedural diagram showing the iteration loop over wavelength. An array of modes, ω_k , is stored for each wavelength, λ_j .

4.4 Mode sorting

In the foregoing configuration of the finite element simulation, we noted the *ad hoc* specification of the boundary conditions for surface waves. Bulk wave resonances will still be found; i.e. the system is underdetermined with respect to surface waves.

To automatically distinguish the surface modes from the bulk modes, we implemented a mode sorting technique using the depth-weighted strain energy. This does not explicitly classify modes, rather the “depth of energy” measure is generally useful because all modes carrying a majority of energy at the surface will produce greater surface displacements and are therefore the most measurable. We validate this against experimental data in a subsequent section.

Like the energy stored in a spring, the strain potential energy is proportional to the square of the displacement. In general, the displacements are now complex due to the Bloch boundary phasor of form: $\exp(i2\pi x/a)$. So our real-valued measure of acoustic energy is proportional to the norm-square of each strain component.

The energy function we employ is the centroid of strain energy along the y (depth) axis of the simulation domain. The following equation shows the computation of “depth of energy,” DOE, using both the x and y directed strains S_x and S_y at every point (x,y) .

$$DOE = y_{\max} - \frac{\iint_D (S_x S_x^* + S_y S_y^*) y \, dx dy}{\iint_D (S_x S_x^* + S_y S_y^*) \, dx dy} \quad (5)$$

In MATLAB code, the computation of the numerator is realized according to the following:

```

ymax = 1.8*lambda(j) + t_layer;
doe_num(j) = ymax - ...
  postint(fem, ['( ux*conj(ux)' ...
    '+ uy*conj(uy) ) * y'], ...
  'solnum', j);
  
```

In results that follow, we use a simple selection criterion: normalize the DOE to the subdomain height, and establish a threshold for relevant modes. We typically ignore modes with normalized DOE greater than 0.2, or 20% of the depth of the simulation domain.

A graphical comparison of the DOE for typical modes is included in Figure 4. Higher order versions of these modes also occur and are included in the results of subsequent sections but are not shown here.

DoE [um]	Frequency [GHz]	Type	
0.5323	1.216	SAW	
2.4478	1.485	LSAW	
3.1441	1.109	Bulk	

Figure 4. Depth of energy comparison for three modes produced by a single eigenfrequency simulation over a silicon subdomain. Vertical displacement surface plots are shown to the right.

In Figure 4 it is clear the modes may be strictly periodic in the x coordinate (SAW, Bulk), or in both x and y coordinates. The latter

case corresponds to a combination of surface and bulk propagation (LSAW).

5. Results

5.1 Dispersion in thin films

The case of acoustic wave dispersion in a thin film over an infinite half-space has been extensively studied by Auld, Solie, and others [6]. We present a structure commonly used to generate acoustic waves in silicon: a piezoelectric zinc oxide layer over a silicon substrate. This configuration recently has been evaluated both experimentally and numerically for some practical acoustic devices [4,5].

For this layered structure, one intuitively expects a transition of behavior: as the acoustic wavelength decreases the wave energy is confined closer to the surface, and the wave “sees” only the film properties. Thus the velocity decreases from that of silicon to that of ZnO as the wavelength decreases (k increases).

We compare our results to those obtained by a Laguerre polynomial method, as shown in Figure 5 and reported by Kim and Hunt in 1990 [7].

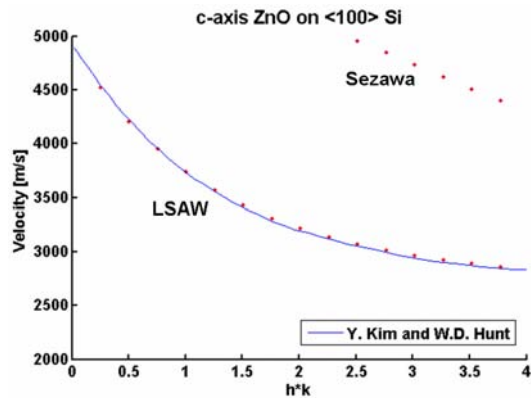


Figure 5. Velocity dispersion diagram for a ZnO layer over a silicon substrate. The wave vector is normalized by layer thickness. Comparison is made to data computed by Laguerre polynomial expansion [7].

Note the mode with greater velocity in Figure 5. This mode is the first generalized Lamb mode which becomes guided in the thin film on the semi-infinite substrate. The

generalized Lamb mode for the thin film / substrate waveguide structure, denoted M_{21} , is commonly called the Sezawa mode [6].

5.2 Dispersion in 1-D thin film PnCs

In this test case, we simulate a structure which Mazav et. al. have fabricated and experimentally examined [8]. This example of a one-dimensional (1D) surface phononic crystal consists of a copper and silicon equal-width line pattern on a silicon substrate. Our modeling of the lattice unit cell for such a structure is shown in the sagittal section plot of Figure 6. The finite element mesh is illustrated by triangles.

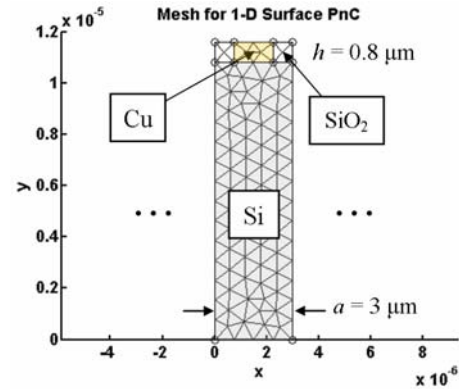


Figure 6. Mesh plot of the computational domain for the unit cell of a surface phononic crystal reported by A. A. Maznev [8].

The lattice constant, or period of structure replication along the x axis, is denoted a . Periodic boundary conditions were applied to all left and right boundaries and vertices (both silicon dioxide and silicon). The periodic constraints were modified to include an additional complex exponential phase factor introducing the solution wavelength, λ , where $k = 2\pi/\lambda$:

$$\begin{aligned} u(x) &= u(x+a) * \exp(ika) \\ v(x) &= v(x+a) * \exp(ika) \end{aligned} \quad (6)$$

After solving according to these constraints, Figure 7 reveals the many modes produced. Each eigenfrequency point is colored according to depth of energy; blue points would indicate

energy at the bottom of the computational domain (impossible given the fixed boundary condition) and red points correspond to surface modes.

Surface wave band gaps appear when energy can no longer propagate with certain k vectors. For example there may exist a range of frequencies (phonon energies) and wave numbers for which surface modes do not exist. This corresponds to a surface phononic band gap in one dimension. If there was instead a range of frequencies for which no surface k vector produced any mode, that would constitute a *complete* surface phononic band gap in one dimension.

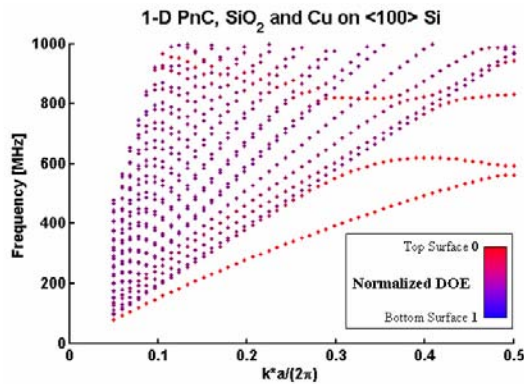


Figure 7. Frequency dispersion of all modes of the phononic crystal structure. Surface modes are shown in red, and bulk modes (diagonal lines of dots) have shades of purple.

This concept can also be extended to 2D and 3D lattices for which the band gap is complete if it also exists for all 2D or 3D propagation directions, respectively.

In Figure 7 the modes which prevent a complete 1D phononic band gap are not pure surface modes, they propagate and radiate energy away from the surface. However, we are interested in the surface modes, so we place a threshold on the surface energy measure, selecting only modes with a normalized DOE < 0.2 . This implies the strain energy centroid is within the top 20% of the total structure height. Figure 8 shows the modes thus selected agree well with measurements from an impulsive laser acoustic spectrometer [8].

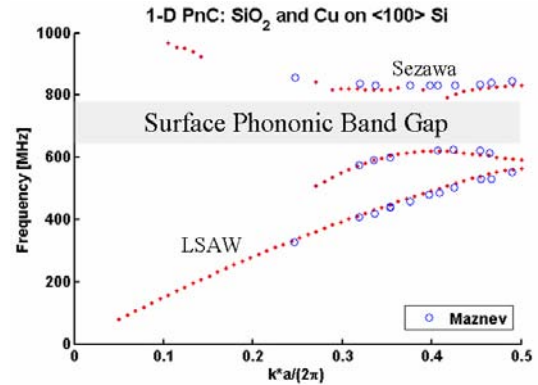


Figure 8. SAW dispersion showing a surface wave band gap along one dimension. FEM simulation (solid dots) and laser probe measurements (open circles) show both leaky SAW and Sezawa modes.

6. Discussion

One of the advantages we notice with FEM is that arbitrary geometries may be handled quite well. Perturbation techniques, however, can only extend a limited range from the given analytical solution.

Several authors such as Tiersten and Solie have already demonstrated numerical results in much better agreement with experiment than perturbative methods [6]. Because our FEM results agree so closely with these other numerical techniques and with at least one physical experiment, we believe this approach is generally more accurate for assessment of arbitrary structures relative to previous treatments accurate in a narrow perturbative range.

Other numerical approaches for solving surface waves in layered structures are common. Several methods in the literature are quite similar in formulation of the eigenproblem specified in this work [7, 9, 10]. In those studies, the inhomogeneous structure is treated differently. Plane wave propagation is typically assumed and the number of degrees of freedom is reduced considerably. In the Laguerre polynomial approach, the polynomial was expanded to order 5, yielding $3(N+1)=18$ eigenmodes [7].

The present study required relatively few degrees of freedom considering a finite element approach. The results still agree well with both theory and experiment. This is also despite the approximation we made: specifying a 1.8

wavelength thick structure to emulate the semi-infinite case. Unfortunately, perfectly matched layers and infinite elements are not available to simulate an infinite depth in this application mode.

Over the many iterations of for production of a dispersion plot, the consistent scaling of the domain corresponding to the acoustic wavelength is important. Keeping such factors constant reduces the chance systematic numerical dispersion could appear as an artifact.

7. Conclusions

We have shown the utility of COMSOL Multiphysics for evaluation of surface acoustic wave dispersion in layered structures of anisotropic materials. We leveraged the eigenfrequency solver of the MEMS Module and its piezoelectric mode in addition to the fully anisotropic material constants in our simulations.

The first simulated structure was a thin piezoelectric zinc oxide film on a single crystal silicon substrate. The FEM dispersion data closely matched the Laguerre polynomial result, confirming its suitability for that case.

Our second simulated structure was a thin film one-dimensional phononic crystal which has previously been experimentally reported [8]. In this case, the thin film had alternating (periodic) material properties in the x direction. We configured the model as a lattice unit cell by assigning periodic boundary conditions, and we varied the solution to show dispersion by modulating the boundary condition with a complex exponential dependent upon the acoustic wavelength.

Without presuming details of the eigenfunctions, we have restricted the solutions to surface modes using a centroid formulation for the depth of acoustic energy. In a final step, we demonstrated the success of the mode sorting procedure to determine modes which are likely to be observed by a laser acoustic spectrometer.

8. References

1. Harshal B. Nemade, et al. Simulation of One-Port SAW Resonator using COMSOL

Multiphysics, *COMSOL Users Conference*, Bangalore (2006)

2. Y.L. Rao, G. Zhang, 3-D Finite Element Simulation of Nanostructure Enhanced SAW Sensors, *COMSOL Users Conference*, Boston, USA (2006)

3. COMSOL AB, SAW Gas Sensor, *technical white paper* (2007)

4. S. Mohammadi, A.A. Eftekhari, A. Khelif, H. Moubchir, R. Westafer, W.D. Hunt and A. Adibi, Complete phononic bandgaps and bandgap maps in two-dimensional silicon phononic crystal plates, *Electronics Letters*, **43**, 16 (2007)

5. S. Mohammadi, A.A. Eftekhari, A. Khelif, W.D. Hunt, and A. Adibi, High-Q micromechanical resonators in a two-dimensional phononic crystal slab, *Applied Physics Letters*, **94**, 1 (2009)

6. B.A. Auld, *Acoustic Fields and Waves in Solids*, Vol. II, pp. {92, 275-285, 102-103}, Krieger Publishing Company, Malabar FL (1990)

7. Y. Kim, W.D. Hunt, A Laguerre Polynomial Approach To Surface Acoustic Wave Propagation In Multilayered Structures, *IEEE Ultrasonics Symposium* (1990)

8. A.A. Maznev, Band gaps and Brekhovskikh attenuation of laser-generated surface acoustic waves in a patterned thin film structure on silicon, *Physical Review B*, **78**, 155323 (2008)

9. E.L. Adler, SAW and Pseudo-SAW Properties Using Matrix Methods, *IEEE Ultrasonics Symposium*, p. 455 (1992)

10. P.M. Smith, Dyadic Green Functions for Multi-layer SAW Substrates, *IEEE Trans. UFFC*, **48**, No. 1 (2001)

9. Acknowledgements

This work was supported by the National Science Foundation under contract no. ECS-0524255 (L. Lunardi) and the Office of Naval Research under contract no. 21066WK (M. Spector).

The authors would like to thank Professor Oliver Brand, Sandra Pierotti, and Matt Blake for their roles in making COMSOL Multiphysics available at Georgia Tech.